

Adsorption isotherm studies of methyl chloride on MgO

Michael Sprung and J. Z. Larese

Chemistry Department, Brookhaven National Laboratory, Upton, New York, 11973-5000

(Received 30 June 1999)

The wetting properties of methyl chloride (CH_3Cl) on MgO (100) surfaces have been investigated between 132 and 180 K using high-resolution adsorption isotherms. At low temperatures only one adsorption step is observed. At higher temperatures, i.e., $T > 158.9$ K, a second isotherm step appears, signaling the presence of a layering transition. Unlike adsorption behavior on graphite, however, there is no evidence of a low-to-high-density transition in the monolayer phase. In addition to the layering properties, the isothermal compressibility and isosteric heat of adsorption of the adsorbed films are calculated.

INTRODUCTION

Much is known about the physisorption of gases on graphite and on close-packed metal surfaces but the number of previous investigations involving MgO (Ref. 1) is more limited. This paper represents the first in a planned series of studies aimed at understanding the adsorption properties of methyl halides (CH_3R , $R = \text{F, Cl, Br, I}$) on MgO. Our goal is to explore the interaction of small, polar, hydrocarbon molecules with ionic surfaces exhibiting four-fold symmetry, i.e., MgO (100) surfaces, and to probe both the details of two-dimensional (2D) electrostatic ordering and film wetting properties. Here, we report high-resolution volumetric adsorption isotherm investigations of the thermodynamic properties of methyl chloride (CH_3Cl) films on MgO extending over a temperature range from 132 to 180 K. It should be noted that numerous experimental techniques, including He atom scattering,² x-ray and neutron diffraction,³⁻⁵ heat capacity,⁶ and volumetric isotherm studies,⁷ have been applied to the study of the adsorption properties of CH_3Cl on graphite. Knorr has presented a comprehensive review of the adsorption properties of all the polar methane derivatives on graphite.⁸ Comparison of the present studies with these earlier investigations should lead to a better understanding of how the interplay of adsorbate-adsorbate and adsorbate-substrate interactions determines the properties of these interesting adsorbed phase systems. The availability of large quantities of highly uniform, crystalline powders of MgO (produced by a novel technique developed in our laboratory) has aided our ability to undertake such investigations. MgO forms a rock salt structure with a (100) surface lattice constant of 2.978 Å. It is also important to realize that MgO powders can be produced with predominantly (100) facets exposed.

EXPERIMENTAL SETUP

The details of our isotherm apparatus and of how we perform our volumetric isotherms can be found elsewhere.⁹ Briefly, approximately 0.4 g of MgO was loaded into an oxygen free high conductivity (OFHC) copper cell and mounted in a closed-cycle helium refrigerator (APD Cryogenics). Successive helium gas expansions were used to determine that the dead space volume of the cell and attached

capillary was a few cm^3 (depending on the exact cell used in the individual experiment). The dead space is weakly temperature dependent. Different pressure sensors (MKS Baratron) were used to guarantee adequate pressure measurement sensitivity over the entire temperature range (132–180 K). The calibrated dosing volumes varied between 55.0 and 60.0 cm^3 because each of the pressure sensors had a slightly different internal and interconnecting volume associated with it. Adsorption cell temperatures were monitored and controlled to ± 3 mK using a commercial temperature controller (Conductus LTC 10).

All of the MgO powders used in these studies were synthesized in our laboratory and had surface areas of approximately 10 m^2/gm . Electron microscopy revealed that the powders consisted of cubic particles, 150–200 nm mean size. They were heat-treated *in vacuo* (final pressure $\leq 2 \times 10^{-7}$ Torr) at 950 °C for 36 h. Loading of MgO powder into the copper sample cell was done in a glove box under a dry argon atmosphere. A methane (CH_4) isotherm was used to check the quality of the powder and determine its monolayer capacity. The adsorbate was liquid phase, 99.9% pure CH_3Cl (Matheson). Before being introduced into the system it was further purified by performing several freeze-thaw distillation cycles.

RESULTS

More than twenty adsorption isotherms were measured in the temperature range $132 < T < 180$ K to determine the wetting properties of CH_3Cl on MgO (a subset of these isotherms is shown in Fig. 1). Our measurements were restricted to temperatures above 132 K because at lower temperatures the vapor pressures were too small to be reliably determined. At each temperature the adsorbed gas quantity is plotted against the reduced pressure (i.e., pressure normalized to the saturated vapor pressure of bulk CH_3Cl at the given temperature). We were able to estimate σ , the molecular cross section of CH_3Cl on the MgO (100) surface, by comparing the monolayer step heights of the CH_3Cl and CH_4 isotherms (CH_4 forms a solid, $\sqrt{2} \times \sqrt{2} R 45^\circ$ commensurate square lattice on MgO (Ref. 10) with each CH_4 molecule occupying 17.74 Å² of (100) surface. At 170.0 K $\sigma = 23.9$ Å² for CH_3Cl on MgO.

Before turning to a detailed analysis of the isotherm data, it will be helpful to make a few general comments concern-

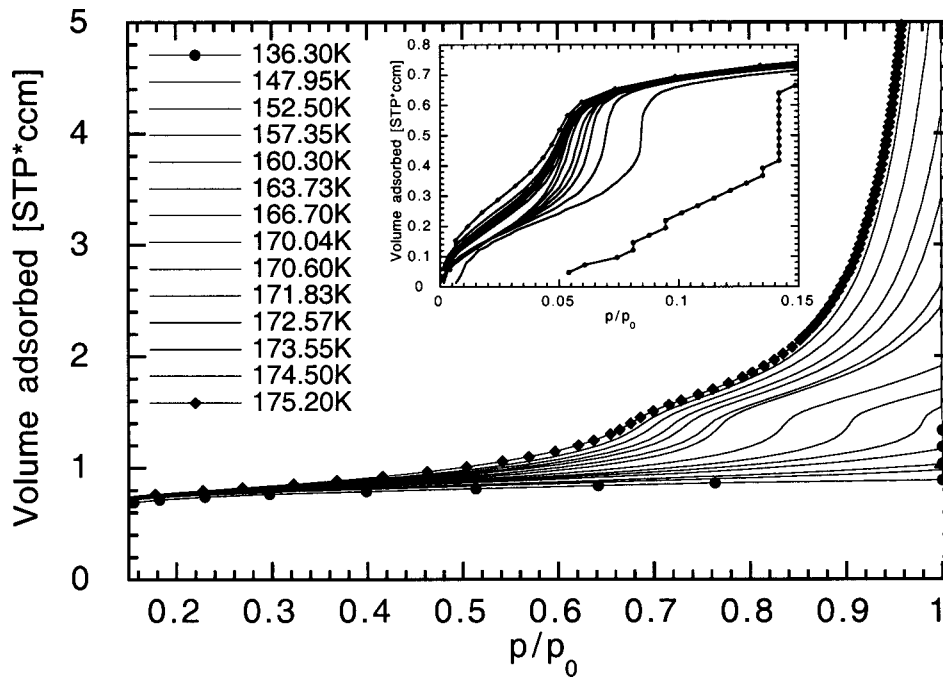


FIG. 1. A subset of Chloromethane on MgO isotherms. The height of the isotherm near $p/p_0=1$ increases with temperature. The inset illustrates the behavior of the isotherms in the monolayer regime ($p/p_0 \leq 0.15$). As noted in the text the vapor pressures at the lowest temperatures (i.e., $T = 136.3$ K and below) are near the resolution of our pressure transducer and A-to-D converter producing the step-wise displacement of the data points.

ing the wetting properties of CH_3Cl on MgO. First of all, several layering/wetting features (as, i.e., the appearance of various steps and changes in the shape of the isotherm as $p/p_0 \rightarrow 1.0$) were observed. Second, at temperatures below 157 K only a single (presumably solid) monolayer film forms before evidence of bulk CH_3Cl formation appears. This behavior is different from CH_3Cl on graphite where first a low-density (LD) and then a high-density (HD) solid monolayer phase forms. On graphite, the LD-to-HD phase transition appears as a distinct substep following a vertical riser in isotherms below 145 K.⁷ No such sub-step appears in the $\text{CH}_3\text{Cl}/\text{MgO}$ isotherms indicating that even if CH_3Cl forms a monolayer solid on MgO no LD-to-HD phase transition takes place. It is relevant to point out that unlike graphite, MgO is an ionic solid and it is not surprising that polar molecules would behave differently on the two substrates. Perhaps, the difference in behavior may be a consequence of a stronger adsorbate(A)-substrate(S) interaction. Unfortunately, Bah and Dupont-Pavlovsky⁷ do not include any information about the relative strength of the A-A and A-S interactions. Third, at higher temperatures a second step appears in the isotherms. By monitoring the position (in reduced pressure units) of this second step we can locate the temperature, $T_{2\text{nd}}$, where this feature first shows up. A linear fit of the position of the second isotherm step (as determined from the peaks in the compressibility vs reduced pressure in Fig. 4) indicates $T_{2\text{nd}} = 158.9$ K. Finally, no evidence of additional discrete (stepwise) layer formation is recorded beyond the second step. Customarily, the terms “nonwetting,” “incomplete,” and “complete” wetting are used to describe different modes of film growth on surfaces.¹¹ The shape of an isotherm near the saturated vapor pressure can be used as a qualitative indicator of which of these wetting modes takes place. When only a finite number of adsorption steps are

visible before the isotherm reaches the saturated bulk vapor pressure (SVP) layering is likely to be “incomplete.” Not infrequently an asymptotic increase in layer thickness is observed near the bulk triple point, T_{triple} . Film growth to a macroscopic thickness at T_{triple} is commonly referred to as triple-point wetting. T_{triple} for CH_3Cl is 175.44 K. Figure 2 displays the film growth as a function of reduced temperature. Even at the highest coverage (limited in this experiment to about 15–20 equivalent layers) the SVP has still not been reached for the isotherms at either 174.50 or 175.20 K. Although it is not possible to unequivocally say that the isotherm data shown in Fig. 2 represent an asymptotic approach to the SVP at $T > 174.5$ K, these data strongly suggest that “complete” wetting takes place at or near T_{triple} .

Frenkel, Halsey, and Hill (FHH)^{12,13,14} proposed that the long range van der Waals interaction between substrate and

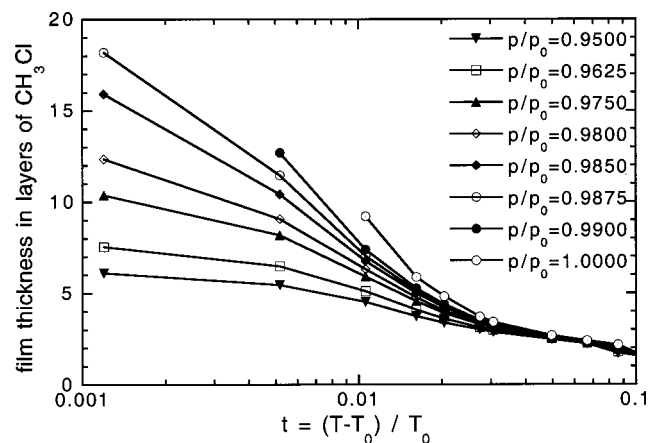


FIG. 2. Film growth of Methyl Chloride on MgO as a function of reduced temperature for different p/p_0 .

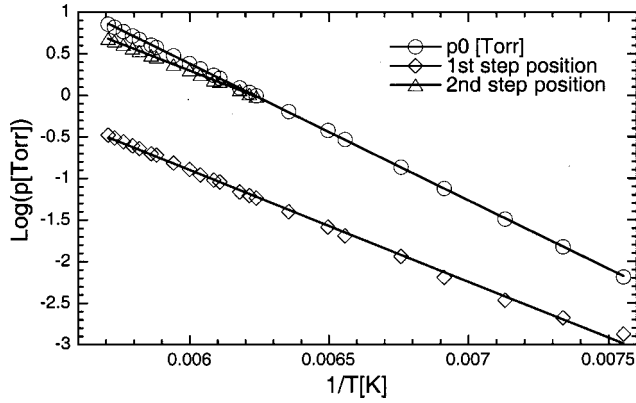


FIG. 3. Variation of vapor pressure of the adsorption steps with temperature. The second layer onset temperature is $T_{2nd} = 158.9$ K.

adsorbate molecules can be used to describe the behavior of thick physisorbed films. Their approach predicts an isotherm shape near saturation of the form:

$$p/p_0 = \exp\left(\frac{-\alpha\beta}{d^s}\right), \quad (1)$$

with $\alpha > 0$, $\beta = (k_B T)^{-1}$, d representing the film thickness and the exponent $s = 3.0$. Fitting the isotherms at 174.50 and 175.20 K to the FHH form we find $s = 2.00$ and $s = 1.28$ respectively. Explanations for the deviations from $s = 3$ could be related to either the limited coverage range of our measurements, or to thermal fluctuations¹⁵ or possibly to the dipole-dipole interaction between the adsorbate molecules.

Larher¹⁶ has shown that the enthalpy and the entropy of the gas and condensed phase can be related to the SVP by

$$R \cdot \ln p_0 = -\frac{(h_g - h_c)}{T} + (s_g - s_c). \quad (2)$$

Using Clapeyron's equation, this can be related to the pressure dependence of the n th step position as a function of temperature

$$\log_{10} p(\text{Torr}) = \frac{-A_n}{T} + B_n. \quad (3)$$

Figure 3 shows the temperature dependence of the bulk vapor pressure and the position of the first and second adsorption steps. Table I lists the coefficients obtained from fits to Eq. (3). Two thermodynamic quantities, the isothermal compressibility and the isosteric heat of adsorption, can be extracted from a set of high-resolution isotherms. As noted in Ref. 17 the two-dimensional isothermal compressibility can be calculated as

TABLE I. Coefficients of the parameters A , B , and R (correlation coefficient) of Clapeyron's equation.

	Sat. vapor pressure	1st step position	2nd step position
A	1648 ± 3 K	1346 ± 15 K	1313 ± 3 K
B	10.27 ± 0.03	7.18 ± 0.09	8.18 ± 0.03
R	0.99997	0.9988	0.99994

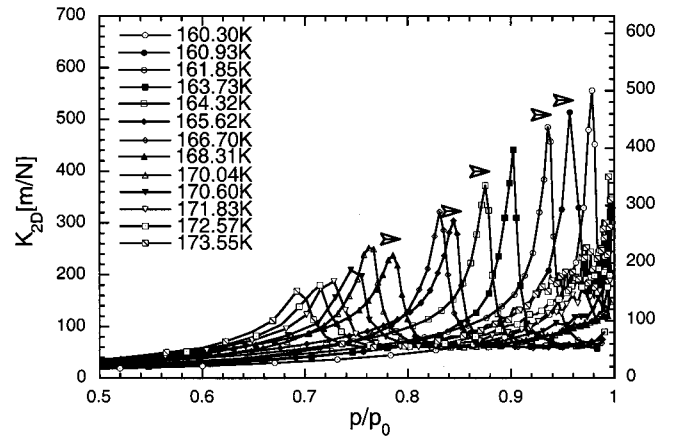


FIG. 4. Two-dimensional compressibility of the second adsorption step of CH_3Cl on MgO for isotherm above T_{2nd} . Note dual scale for compressibility values. Arrows indicate correct vertical scale to use for individual compressibility traces.

$$K_{2D} = \frac{A}{N_A \cdot k_B \cdot T} \cdot \frac{p}{N_{ads}^2} \cdot \frac{dN_{ads}}{dp}, \quad (4)$$

where A is the surface area of the sample in m^2 , p is the vapor pressure in N/m^2 , T the temperature in K, N_A is Avogadro's number, k_B is Boltzmann's constant, and N_{ads} is the number of molecules adsorbed. Since layer formation is accompanied by a change in isothermal compressibility, changes in the compressibility can be used to identify layering transitions.

Figure 4 shows the 2D isothermal compressibility for reduced pressures, p/p_0 , between 0.5 and 1. The compressibility peak is associated with second-layer formation. With increasing temperature this feature moves toward lower reduced pressure, decreases in height and broadens in width. This behavior can be related to an increase in the mobility of the molecules within the layer and a corresponding loss in long range order (i.e., with fluidlike properties).

It is not possible to make as comprehensive an analysis of the isothermal compressibility of the first layer mainly because the vapor pressure is low. But even though the monolayer data are statistically less reliable, they are good enough to establish that the first layer behaves qualitatively very much like the second in terms of how the compressibility feature decreases in height, broadens and moves with increases in temperature.

The second thermodynamic quantity that can be extracted from a set of closely spaced isotherms is the isosteric heat of adsorption. This quantity represents the work required to bring one molecule from the 3D vapor into the 2D film. It can be determined using:

$$Q_{st} = RT^2 \cdot \left. \frac{\partial \ln p}{\partial T} \right|_x. \quad (5)$$

The calculated heat of adsorption for a subset of the isotherms is shown in Fig. 5 below. It converges towards $Q_{st} = (7.5 \pm 0.3)$ kcal/mole at high coverage. The behavior of Q_{st} for the highest temperature isotherm does not appear to converge towards the value quoted above. However, a closer inspection of the data, especially as one approaches T_{triple} is

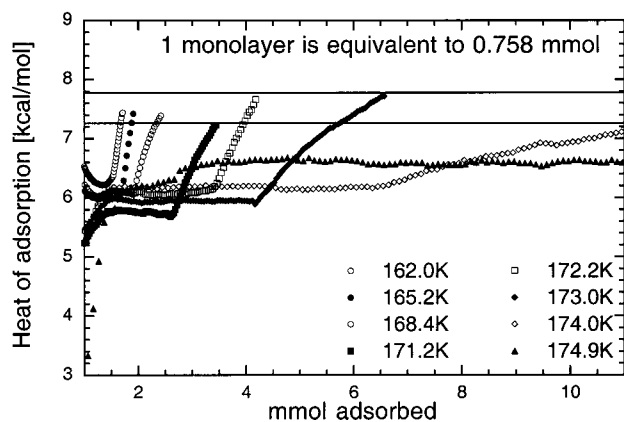


FIG. 5. Isosteric heat of adsorption from CH_3Cl on Magnesium Oxide.

needed. Notice that several of Q_{st} plots exhibit a plateau near 6 kcal/mole and, with increasing coverage, approach 7.5 ± 0.3 kcal/mol more slowly as $T \rightarrow T_{\text{triple}}$. It should be noted that the isotherms at 174.0 and 174.9 K, where this trend is clearly visible, are also the two isotherms where “complete” wetting takes place. Bah and Dupont-Pavlovsky⁷ have not included a determination of Q_{st} for CH_3Cl on graphite so no comparison is possible.

The heat of vaporization of bulk CH_3Cl is reported as 5.14 kcal/mole (Ref. 18) at the equilibrium saturation vapor pressure of 1 atm. In Ref. 19 the heat of vaporization was determined over the temperature range from -28.89 to 37.78 °C. Over this interval it varied from 5.23 to 4.38 kcal/mole. Our measurements were done at much lower tempera-

tures and pressures, so a comparison with these values is not possible. Nevertheless, it appears that the trend is consistent with the values we determined.

CONCLUSION

The adsorption of CH_3Cl on MgO (100) surfaces exhibits several interesting layering properties within the 132–180 K temperature range. A second adsorbed layer forms at temperature above $T_{2\text{nd}} = 158.9$ K and the wetting behavior changes from “incomplete” to “complete” near the triple point. Similar layering and wetting behavior has been observed for NH_3 films on MgO (Ref. 17) where $T_{2\text{nd}}$ was also about $0.9T_{\text{triple}}$ and where complete wetting also appears to take place in the neighborhood of T_{triple} .

Evidently, the interaction between the ionic MgO surface and the polar CH_3Cl molecule is too strong to allow a density-dependent, LD-to-HD monolayer transition to occur as was seen in the CH_3Cl on graphite system. This observation is supported by our recent x-ray diffraction studies of CH_3I on MgO .²⁰ Future investigations using elastic and inelastic neutron diffraction techniques are planned to obtain a more complete understanding of the structural and dynamical properties of the CH_3Cl on MgO system.

ACKNOWLEDGMENTS

We are pleased to acknowledge the skilled help of C. Koehler and D. Becker. It is also a pleasure to acknowledge useful discussions with B. Asmussen, A. Freitag, J. Hastings, W. Kunnmann, and L. Passell. This work was supported by the U.S. Department of Energy, Materials Science Division under Contract No. DE-AC02-98CH10886.

¹L. W. Bruch, M. W. Cole, and E. Zaremba, *Physical Adsorption Forces and Phenomena* (Oxford University Press, New York, 1997) and references therein.

²J. C. Ruiz-Suarez *et al.*, *Phys. Rev. Lett.* **61**, 710 (1988).

³A. R. B. Shirazi and K. Knorr, *Surf. Sci.* **243**, 303 (1991).

⁴K. Morishige, Y. Tajima, S. Kittaka, S. M. Clarke, and R. K. Thomas, *Mol. Phys.* **72**, 395 (1991).

⁵S. Grieger and W. Press, *Europhys. Lett.* **33**, 193 (1996).

⁶A. Inaba and H. Chihara, *J. Phys. Soc. Jpn.* **60**, 17 (1991).

⁷A. Bah and N. Dupont-Pavlovsky, *Surf. Sci.* **338**, 293 (1995).

⁸K. Knorr, *Phys. Rep.* **214**, 114 (1992).

⁹Z. Mursic, M. Y. Lee, D. E. Johnson, and J. Z. Larese, *Rev. Sci. Instrum.* **67**, 1886 (1996).

¹⁰J. P. Coulomb, K. Madih, B. Croset, and H. J. Lauter, *Phys. Rev. Lett.* **54**, 1536 (1985).

¹¹See, e.g., M. Schick, in *Liquids at Interfaces*, edited by J.

Charvolin, J. F. Joanny, and J. Zinn-Justin (Elsevier, Amsterdam, 1990) and references therein.

¹²J. Frenkel, *Kinetic Theory of Liquids* (Clarendon, Oxford, 1946).

¹³G. D. Halsey, Jr., *J. Chem. Phys.* **16**, 931 (1948); **17**, 520 (1949).

¹⁴T. L. Hill, *J. Chem. Phys.* **17**, 590 (1949); **17**, 668 (1949); *Adv. Catal.* **4**, 211 (1952).

¹⁵K. R. Mecke and J. Krim, *Phys. Rev. B* **53**, 2073 (1996).

¹⁶Y. Larher, in *Surface Properties of Layered Structures*, edited by G. Benedek (Kluwer, Dordrecht, 1992), p. 261.

¹⁷D. E. Johnson and J. Z. Larese, *Phys. Rev. B* **59**, 8247 (1999).

¹⁸F. D. Rossini, D. D. Wagman, W. H. Evans, S. Levine, and I. Jaffe, *NBS Circ.* 500 (1952).

¹⁹CRC, *Handbook of Chemistry of Physics*, 46th ed., Table E 19.

²⁰See, e.g., J. Z. Larese *et al.*, National Synchrotron Light Source, July 1999, Newsletter, p. 4; and M. Sprung and J. Z. Larese (to be published).